$\eta \to \pi^0\gamma\gamma$ decay within a chiral unitary approach

E. Oset[1], J. R. Peláez[2] and L. Roca[1]

[1] *Departamento de Física Teórica and IFIC Centro Mixto Universidad de Valencia-CSIC Institutos de Investigación de Paterna, Apdo. correos 22085, 46071, Valencia, Spain*

[2] *Dip. di Fisica. Universita' degli Studi, Firenze, and INFN, Sezione di Firenze, Italy Departamento de Física Teórica II, Universidad Complutense. 28040 Madrid, Spain.*

Abstract

We improve the calculations of the $\eta \to \pi^0\gamma\gamma$ decay within the context of meson chiral lagrangians. We use a chiral unitary approach for the meson-meson interaction, thus generating the $a_0(980)$ resonance and fixing the longstanding sign ambiguity on its contribution. This also allows us to calculate the loops with one vector meson exchange, thus removing a former source of uncertainty. In addition we ensure the consistency of the approach with other processes. First, by using vector meson dominance couplings normalized to agree with radiative vector meson decays. And, second, by checking the consistency of the calculations with the related $\gamma\gamma \to \pi^0\eta$ reaction. We find an $\eta \to \pi^0\gamma\gamma$ decay width of 0.47 ± 0.10 eV, in clear disagreement with published data but in remarkable agreement with the most recent measurement.

1 Introduction

The $\eta \to \pi^0\gamma\gamma$ decay has attracted much theoretical attention, since Chiral Perturbation Theory (ChPT) calculations have sizable uncertainties and produce systematically rates about a factor of two smaller than experiment [1, 2]. In contrast models using quark box diagrams [3, 4] claim to obtain acceptable rates. Within ChPT, the problem stems from the fact that the tree level amplitudes, both at $O(p^2)$ and $O(p^4)$, vanish. The first non-vanishing contribution comes at $O(p^4)$, but either from loops involving kaons, largely suppressed due to the kaon masses, or from pion loops, again suppressed since they violate G parity and are thus proportional to $m_u - m_d$ [5]. The first sizable contribution comes at $O(p^6)$ but the coefficients involved are not precisely determined. One must recur to models: either Vector Meson Dominance (VMD) [5, 6, 7], the Nambu-Jona-Lasinio model (NJL) [8], or the extended Nambu-Jona-Lasinio model (ENJL) [9, 10], have been used to determine these parameters. However, the use of tree level VMD to obtain the $O(p^6)$ chiral coefficients by expanding the vector meson propagators, leads [5] to results about a factor of two smaller than the "all order" VMD term, which means keeping the full vector meson propagator. All this said, the chiral approach has been useful to unveil the physical mechanisms responsible for this decay, but it has become clear that the strict chiral counting has to be abandoned since the $O(p^6)$ and higher orders involved in the full ("all order") VMD results are larger than those of $O(p^4)$. For a review, see [11], together with an experimental upper bound.

Once the "all order" VMD results is accepted as the dominant mechanism, one cannot forget the tree level exchange of other resonances around the 1 GeV region. In comparison with VMD, the exchange of $J^{PC} = 1^{+-}$ axial vectors [12, 13] yields negligible contributions when using values of the couplings in agreement with $\gamma\gamma \to \pi^0\pi^0$ data [14]. Still at tree level, the $a_0(980)$ exchange, which was taken into account approximately in [5], was one of the main sources of uncertainty, since even the sign of its contribution was unknown.

After the tree level light resonance exchange have been taken into account, we should consider loop diagrams, since meson-meson interaction or rescattering can be rather strong. First of all we find the already commented $O(p^4)$ kaon loops from ChPT, but also the meson loops from the terms involving the exchange of one resonance. The uncertainty from the latter was roughly expected [5] to be about 30% of the full width.

Another relevant question is that no attempts have been done to check the consistency of $\eta \to \pi^0\gamma\gamma$ results with data from other processes. On the one hand, the decay results have not been compared with the crossed channel $\gamma\gamma \to \pi^0\eta$, although some consistency tests with $\gamma\gamma \to \pi^0\pi^0$ have been carried out as quoted above. The reason is not surprising since there are no hopes within ChPT to reach the $a_0(980)$ region where there are measurements of the $\gamma\gamma \to \pi^0\eta$ cross section [15, 16]. On the other hand, the explicit SU(3) breaking already present in the radiative vector meson decays has not been taken into account when calculating the VMD tree level contributions.

The former discussion has set the stage of the problem and the remaining uncertainties that allow for further improvement. In recent years, with the advent of unitarization methods, it has been possible to extend the results of ChPT to higher energies where the perturbative expansion breaks down and to generate resonances up to 1.2 GeV [17, 18, 19, 20, 21, 22]. In particular these ideas were used to describe the $\gamma\gamma \to meson - meson$ reaction, with good results in all the channels up to energies of around 1.2 GeV [23]. Work in a similar direction for this latter reaction has also been done in [24, 25, 26]. With these techniques, and always within the context of meson chiral lagrangians, we will address three of the problems stated above: First, the $a_0(980)$ contribution, second, the evaluation of meson loops from VMD diagrams and, third, the consistency with the crossed channel $\gamma\gamma \to \pi^0\eta$. In particular, we will make use of the results in [23], where the $\gamma\gamma \to \pi^0\eta$ cross section around the $a_0(980)$ resonance was well reproduced using the same input as in meson meson scattering, without introducing any extra parameters.

With these improvements we are then left with a model that includes the "all order" VMD and resummed chiral loops. We expect this approach to provide a good description of $\eta \to \pi^0\gamma\gamma$ because recent studies on the vector meson decay into two pseudoscalar mesons and one photon [27, 28, 29] indicate that such a combination of "all order" VMD contribution plus the unitary summation of the chiral loops leads to good agreement with data in a variety of reactions. These include $\phi \to \pi^0\pi^0\gamma$ [29], where the chiral loops are dominant, $\omega \to \pi^0\pi^0\gamma$ [27, 28], where the VMD mechanism is dominant, and $\rho \to \pi^0\pi^0\gamma$ [27, 28] where both mechanisms have about the same strength.

Concerning the fourth issue of the SU(3) breaking present in radiative vector meson decays, we will take it into account here by using effective couplings normalized to reproduce the most recent experimental data.

Incidentally, there are preliminary results from a very recent experiment [30], which give a decay width about half of the previous one. In that work the authors refined the background subtraction, which was known to be rather problematic. Let us remark that, in view of the former discussion, revisiting the previous theoretical calculations is

mandatory regardless of whether these new experimental results are confirmed or not.

In what follows we will address all these theoretical issues in detail, including an updated estimation of the uncertainties in the calculation. In particular, we will take into account the experimental errors in the radiative vector meson decays, which were neglected before, although they will turn out to be the largest source of uncertainty.

2 VMD contribution

Following [5] we consider the VMD mechanism of Fig. 1 which can be easily derived from

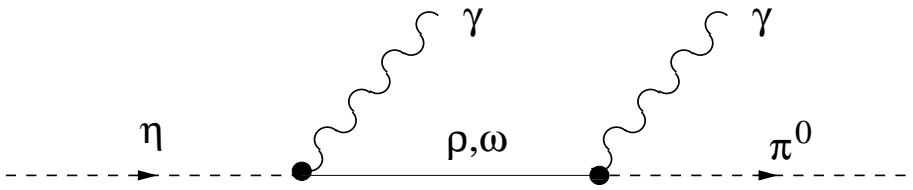

Figure 1: Diagrams for the VMD mechanism.

the VMD Lagrangians involving VVP and $V\gamma$ couplings [33]

$$\mathcal{L}_{VVP} = \frac{G}{\sqrt{2}}\epsilon^{\mu\nu\alpha\beta}\langle\partial_\mu V_\nu \partial_\alpha V_\beta P\rangle, \qquad \mathcal{L}_{V\gamma} = -4f^2 e g A_\mu \langle Q V^\mu\rangle, \tag{1}$$

where V_μ and P are standard $SU(3)$ matrices constructed with the nonet of vector mesons containing the ρ, and the nonet of pseudoscalar mesons containing the π, respectively. For instance for pseudoscalar mesons $P = \tilde{P} + \frac{1}{\sqrt{3}}\eta_1$, with $\tilde{P}$ given by [31]

$$\tilde{P} = \begin{pmatrix} \frac{1}{\sqrt{2}}\pi^0 + \frac{1}{\sqrt{6}}\eta_8 & \pi^+ & K^+ \\ \pi^- & -\frac{1}{\sqrt{2}}\pi^0 + \frac{1}{\sqrt{6}}\eta_8 & K^0 \\ K^- & \overline{K}^0 & -\frac{2}{\sqrt{6}}\eta_8 \end{pmatrix}, \tag{2}$$

and similarly for vector mesons [32]. We also assume the ordinary mixing for the ϕ, the ω, the η and η':

$$\begin{aligned} \omega &= \sqrt{\frac{2}{3}}\omega_1 + \sqrt{\frac{1}{3}}\omega_8, \qquad \phi = \sqrt{\frac{1}{3}}\omega_1 - \sqrt{\frac{2}{3}}\omega_8, \\ \eta &= \frac{1}{3}\eta_1 + \frac{2\sqrt{2}}{3}\eta_8, \qquad \eta' = \frac{2\sqrt{2}}{3}\eta_1 - \frac{1}{3}\eta_8. \end{aligned} \tag{3}$$

In Eq. (1) $G = \frac{3g^2}{4\pi^2 f}$, $g = -\frac{G_V M_\rho}{\sqrt{2}f^2}$ [33] and $f = 93\,\mathrm{MeV}$, with G_V the coupling of ρ to $\pi\pi$ in the normalization of [32]. ¿From Eq. (1) one can obtain the radiative widths for $V \to P\gamma$, which are given by

$$\Gamma_{V\to P\gamma} = \frac{3}{2}\alpha C_i^2 \left(G\frac{2}{3}\frac{G_V}{M_V}\right)^2 k^3, \tag{4}$$

where k is the photon momentum for the vector meson at rest and C_i are $SU(3)$ coefficients that we give in Table 1 for the different radiative decays, together with the theoretical

i	C_i	B_i^{th}	B_i^{exp}
$\rho\pi^0\gamma$	$\sqrt{\frac{2}{3}}$	7.1×10^{-4}	$(7.9\pm2.0)\times10^{-4}$
$\rho\eta\gamma$	$\frac{2}{\sqrt{3}}$	5.7×10^{-4}	$(3.8\pm0.7)\times10^{-4}$
$\omega\pi^0\gamma$	$\sqrt{2}$	12.0%	$8.7\pm0.4\%$
$\omega\eta\gamma$	$\frac{2}{3\sqrt{3}}$	12.9×10^{-4}	$(6.5\pm1.1)\times10^{-4}$
$\phi\eta\gamma$	$\frac{2}{3}\sqrt{\frac{2}{3}}$	0.94%	$1.24\pm0.10\%$
$\phi\pi^0\gamma$	0	–	–
$\begin{matrix}K^{*+}\to K^+\gamma\\ K^{*-}\to K^-\gamma\end{matrix}$	$\frac{\sqrt{2}}{3}(2-\frac{M_\omega}{M_\phi})$	13.3×10^{-4}	$(9.9\pm0.9)\times10^{-4}$
$\begin{matrix}K^{*0}\to K^0\gamma\\ \overline{K}^{*0}\to\overline{K}^0\gamma\end{matrix}$	$-\frac{\sqrt{2}}{3}(1+\frac{M_\omega}{M_\phi})$	27.3×10^{-4}	$(23\pm2)\times10^{-4}$

Table 1: SU(3) C_i coefficients together with theoretical and experimental branching ratios for different vector meson decay processes.

(using $G_V = 69\,\mathrm{MeV}$ and $f = 93\,\mathrm{MeV}$) and experimental [2] branching ratios. We shall refer to these results as those with "universal couplings".

The agreement with the data is fair but the results can be improved by incorporating $SU(3)$ breaking mechanisms [34]. For that purpose, we will normalize here the C_i couplings so that the branching ratios in Table 1 agree with experiment. These will be called results with "normalized couplings". In this way we are taking into account phenomenologically the corrections to the $VP\gamma$ vertex from an underlying field theory.

Once the $VP\gamma$ couplings have been fixed, we can use them in the VMD amplitude corresponding to the diagram of Fig. 1, which is given by

$$\begin{aligned} -it^{VMD} &= \{i\sqrt{6}\frac{1}{q^2-M_\rho^2+iM_\rho\Gamma(q^2)}\left(G\frac{2}{3}e\frac{G_V}{M_\rho}\right)^2\cdot\begin{vmatrix} q\cdot q & q\cdot k_2 & q\cdot\epsilon_2\\ k_1\cdot q & k_1\cdot k_2 & k_1\cdot\epsilon_2\\ \epsilon_1\cdot q & \epsilon_1\cdot k_2 & \epsilon_1\cdot\epsilon_2\end{vmatrix}\\ &\quad +(k_1\leftrightarrow k_2,\, q\to q')\} + \{\rho\to\omega\}, \end{aligned} \tag{5}$$

where $q = P-k_1$, $q' = P-k_2$, with P, k_1, k_2 the momentum of the η and the two photons. We have parametrized the ρ width phenomenologically as: $\Gamma_\rho(q,s) = \frac{(6.14)^2}{48\pi s}(s^2-4s\,m_\pi^2)^{3/2}$ whereas for the ω we have considered a constant $\Gamma_\omega = 8.44$ MeV. Nevertheless, our results are rather insensitive to these details. From the above amplitude, the η decay width is easily calculated, as well as the $\gamma\gamma$ invariant mass distribution

$$\frac{d\Gamma}{dM_I} = \frac{1}{16(2\pi)^4 m_\eta^2}M_I\int_0^{m_{\eta-\omega}}dk_1\int_0^{2\pi}d\phi\;\;\Theta(1-A^2)\,\Sigma\mid t\mid^2, \tag{6}$$

where we take for reference the momentum of the pion, $\vec{p}$, in the z direction, so that

$$\vec{p} = p\begin{pmatrix}0\\0\\1\end{pmatrix},\quad \vec{k_1} = k_1\begin{pmatrix}sin\,\theta\;\cos\,\phi\\ sin\,\theta\;sin\,\phi\\ cos\,\theta\end{pmatrix},\quad \vec{k_2} = -(\vec{k_1}+\vec{p}), \tag{7}$$

$$p = \frac{\lambda^{1/2}(m_\eta^2, M_I^2, m_\pi^2)}{2m_\eta},\quad A\equiv cos(\gamma_1\pi^0) = \frac{1}{2k_1p}[(m_\eta-\omega-k_1)^2-k_1^2-|\vec{p}|^2] \tag{8}$$

with ω the energy of the π^0.

In Fig. 2 we show the results of the mass distribution with and without the radiative widths normalization factors. The integrated width is given by $\Gamma = 0.57\,\mathrm{eV}$ (universal couplings); $\Gamma = 0.30 \pm 0.06\,\mathrm{eV}$ (normalized couplings), where the error has been calculated from a Monte Carlo Gaussian sampling of the normalization parameters within the errors of the experimental branching ratios of Table 1. Let us note that there have been stable values for the vector meson radiative widths throughout the last decade in the PDG but a sizable change in the PDG2002. Had we used the PDG2000, we would have obtained $0.21 \pm 0.05\,\mathrm{eV}$ (normalized couplings).

It is interesting to compare these results with those in [5], where they used a universal SU(3) coupling with G_V adjusted to the $\omega \to \pi^0\gamma$ decay data existing at that time, and obtained an "all orders" value of 0.31 eV. The difference between that value and the $0.21 \pm 0.05\,\mathrm{eV}$ that we would have obtained with older data has to be attributed to the adjusting to all the branching ratios, instead of just one as in [5].

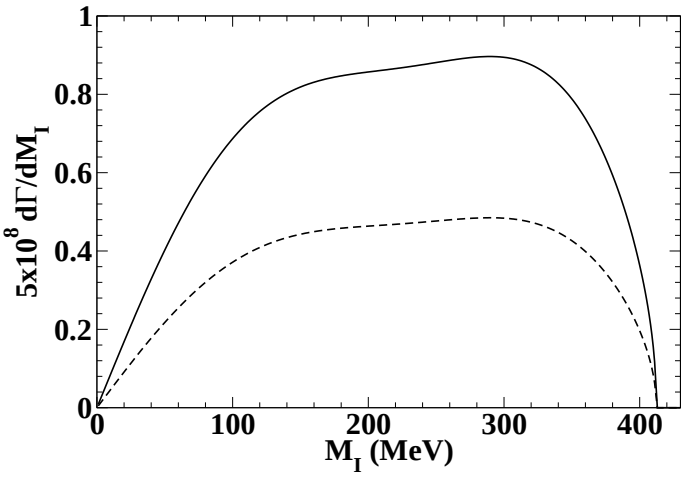

Figure 2: Invariant mass distribution of the two photons with VMD terms only. The solid curve has been calculated with an universal coupling, whereas the dashed one has the couplings normalized differently to fit the radiative decays.

Our VMD normalized result is within three standard deviations from the value presently given in [1],[2]: $\Gamma = 0.84 \pm 0.18\,\mathrm{eV}$, but within one sigma of the more recent one presented in [30], $\Gamma = 0.42 \pm 0.14\,\mathrm{eV}$. There are, however, other contributions that we consider next.

3 Meson loops

The contribution of pion loops to $\eta \to \pi^0\gamma\gamma$, evaluated in [5], proceeds, to begin with, through the G-parity violating $\eta \to \pi^0\pi^+\pi^-$ process. Since the contribution is proportional to $m_u - m_d$, it is very small and we think that if such terms are included, other isospin violating terms proportional to $m_u - m_d$, and isospin violating corrections to the main terms should also be included. Rather than undertaking this delicate task, we will use the results of [5] to estimate uncertainties from all these sources.

The main meson loop contribution comes from the charged kaon loops, calculated at $O(p^4)$ in [5, 8, 9, 10, 12, 14], and proceeds via $\eta \to \pi^0 K^+ K^- \to \pi^0\gamma\gamma$. Note that these loops are also suppressed due to the large kaon masses. That is why the $\eta \to \pi^0 a_0(980) \to$

$\pi^0\gamma\gamma$ mechanism was included explicitly, with uncertainties in the size and sign of the $a_0(980)$ couplings. As commented in the introduction, the chiral unitary approach solves this problem by generating dynamically the $a_0(980)$ in the $K^+K^- \to \pi^0\eta$ amplitude.

In this section, we will illustrate this approach by revisiting the work done in [23] on the related process $\gamma\gamma \to \pi^0\eta$ where the chiral unitary approach was successfully applied around the $a_0(980)$ region. Since for the η decay the low energy region of $\gamma\gamma \to \pi^0\eta$ is also of interest, we will include next the VMD mechanisms also in this reaction. Once we check that we describe correctly $\gamma\gamma \to \pi^0\eta$, the results can be easily translated to the eta decay. We will finally add other anomalous meson loops that are numerically relevant for eta decay but not for $\gamma\gamma \to \pi^0\eta$.

3.1 The unitarized $\gamma\gamma \to \pi^0\eta$ amplitude in the $a_0(980)$ region

In [23] it was shown that, within the unitary chiral approach, the $\gamma\gamma \to \pi^0\eta$ amplitude around the $a_0(980)$ region, diagrammatically represented at one loop in Fig. 3, factorizes as

$$-it = (\tilde{t}_{\chi K} + \tilde{t}_{AK^+K^-})t_{K^+K^-,\pi^0\eta} \tag{9}$$

with $t_{K^+K^-,\pi^0\eta}$ the full $K^+K^- \to \pi^0\eta$ transition amplitude.

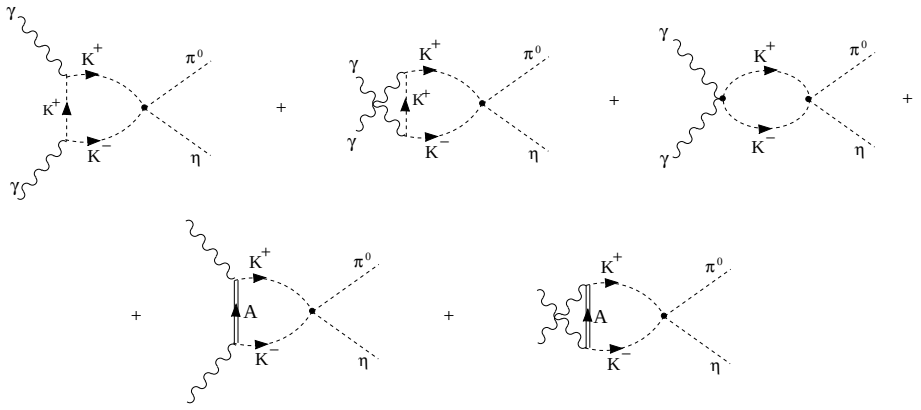

Figure 3: Diagrams for the chiral loop contribution

The first three diagrams correspond to $\tilde{t}_{\chi K}\, t_{K^+K^-,\pi^0\eta}$ of Eq. (9), already evaluated at one loop in [35, 36], where the factorization of the leading $t_{K^+K^-,\pi^0\eta}$ also occurred. In our case $\tilde{t}_{\chi K}$, written in a general gauge to be also used for the $\eta \to \pi^0\gamma\gamma$ reaction, is given by

$$\tilde{t}_{\chi K} = -\frac{2e^2}{16\pi^2}\left(g^{\mu\nu} - \frac{k_{2\mu}k_{1\mu}}{k_1\cdot k_2}\right)\epsilon_{1\mu}\epsilon_{2\mu}\left\{1 + \frac{m_K^2}{s}\left[\log\left(\frac{1+(1-4m_K^2/s)^{\frac{1}{2}}}{1-(1-4m_K^2/s)^{\frac{1}{2}}}\right) - i\pi\right]^2\right\}, \tag{10}$$

above the K^+K^- threshold, with the $-i\pi$ term removed below threshold. Note that the unitarized $t_{K^+K^-,\pi^0\eta}$ transition matrix, not just the lowest order chiral amplitude, is factorized outside the loop integral. This on shell factorization was shown in [23] by proving that the off shell part of the meson-meson amplitude did not contribute to the loop integral.

The meson meson scattering amplitude was evaluated in [17] by summing the Bethe Salpeter (BS) equation with a kernel formed from the lowest order meson chiral Lagrangian amplitude and regularizing the loop function with a three momentum cut off. Subsequently, other approaches like the inverse amplitude method [19, 22] or the N/D method [20] were used and all of them gave the same results in the meson scalar sector. For $\gamma\gamma \to \pi^0\eta$ below 1 GeV only the $L = 0$, $I = 1$ amplitudes are needed [37]. The BS equation sums the diagrammatic series of Fig. 4, which implies that in the $\gamma\gamma \to \pi^0\eta$

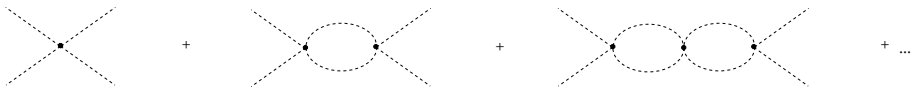

Figure 4: Diagrams summed in the BS equation, using the $O(p^2)$ ChPT vertices.

transition of Fig. 3 one is resumming the diagrams of Fig. 5. Furthermore, the same

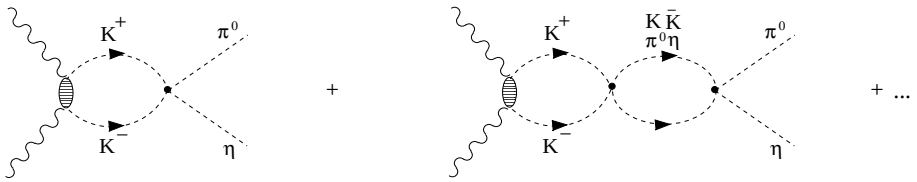

Figure 5: Resummation for $\gamma\gamma \to \pi^0\eta$.

on-shell factorization of the t matrix in the loops found for $\gamma\gamma \to \pi^0\eta$ was also justified for meson-meson scattering in [17]. Thus, the BS equation with coupled channels can be solved algebraically, leading to the following solution in matrix form

$$t(s) = [1 - t_2(s)G(s)]^{-1}t_2(s), \tag{11}$$

with s the invariant mass of the two mesons, t_2 the lowest order chiral amplitude and $G(s)$ a diagonal matrix, $\mathrm{diag}(G_{\overline{K}K}, G_{\eta\pi})$, accounting for the loop functions of two mesons. These G functions were regularized in [17] by means of a cut off. The G analytic expressions, both using a cut off or dimensional regularization can be found in [20].

In Eq. (9) there is another term, $\tilde{t}_{AK^+K^-}t_{K^+K^-,\pi^0\eta}$, which corresponds to the last two diagrams of Fig. 3 where the axial vector meson $K_1(1270)$ is exchanged. For the one loop result we follow [38]. Given the large mass of the axial vector, both the factorization of the unitarized on shell meson-meson scattering amplitude outside the loop, as well as that of the $\gamma\gamma \to K^+K^-$ amplitude are also justified [23]. Hence, when the full series of Fig. 5 is considered, one obtains the contribution $\tilde{t}_{AK^+K^-}t_{K^+K^-,\pi^0\eta}$ with $\tilde{t}_{AK^+K^-}$ given by

$$\tilde{t}_{AK^+K^-} = -2e^2\left(g^{\mu\nu} - \frac{k_{2\mu}k_{1\mu}}{k_1\cdot k_2}\right)\epsilon_{1\mu}\epsilon_{2\mu}\frac{(L_9^r + L_{10}^r)}{f^2}\left[\frac{s_A}{2\beta(s)}ln\left(\frac{1+\beta(s)+\frac{s_A}{s}}{1-\beta(s)+\frac{s_A}{s}}\right) + s\right]\cdot G_{K\overline{K}}, \tag{12}$$

with $s_A = 2(m_A^2 - m_K^2)$, and $\beta(s) = (1 - \frac{4m_K^2}{s})^{1/2}$.

First of all we show in Fig. 6 the result for the $\gamma\gamma \to \pi^0\eta$ cross section obtained from Eq. (9), which coincides with that obtained in [23]. To ease the comparison with experimental data we also show the events concentrated in bins of 40 MeV, roughly like

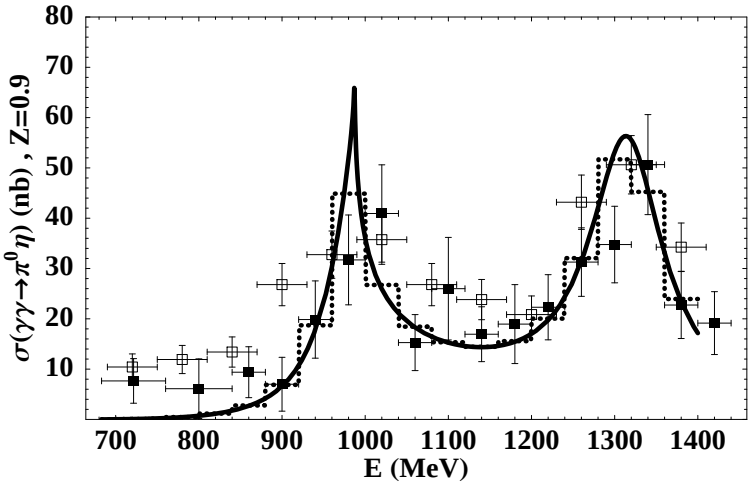

Figure 6: $\gamma\gamma \to \pi^0\eta$ cross section, using Eq. (9). Z is the maximum value of $cos(\theta)$ integrated. The experimental data come from [39, 40], the latter ones normalized in the $a_2(1320)$ peak region. The dashed histogram corresponds to the convolution over an experimental resolution of 40 MeV.

the experimental ones. We can easily notice the peak of the $a_0(980)$ whose dynamical generation is guaranteed by the resummation of diagrams in Fig. 5. The resummed $t_{K^+K^-\to\pi^0\eta}$ amplitude has indeed a pole in the complex plane associated to the $a_0(980)$ resonance [17].

In Fig. 6, we also show results above and below $a_0(980)$, whose description requires further ingredients than those needed just for the $a_0(980)$ region. In particular, the $a_2(1320)$ resonance (second peak) is included phenomenologically as in ref. [23].

In [23] loops like those in Fig. 3, but exchanging a vector meson instead of an axial-vector meson were estimated negligible in the $a_0(980)$ region and hence neglected. In addition, the VMD tree level mechanism of Fig. 1 (with an outgoing η) was neglected since it has no resonant structure in the $\gamma\gamma$ s-channel. As a consequence the agreement of Eq. (9) with experiment is fair but some discrepancies can be noticed in Fig. 6 at low energies.

3.2 VMD mechanisms in $\gamma\gamma \to \eta\pi^0$

For the purpose of the present work, $\eta \to \pi^0\gamma\gamma$, the low energy region of the $\gamma\gamma \to \pi^0\eta$ reaction is also relevant. Therefore we will include as a novelty both the VMD tree level contribution as well as the loops involving vector meson exchange.

First, we can see in Fig. 7 that the results obtained adding the tree level VMD amplitude normalized to the ω, ρ radiative decay rates (dashed line) are acceptable around and below the peak of the $a_0(980)$ resonance. Let us note that the inclusion of these terms does improve the description of the low energy region. The binning of the theoretical results would make again the apparent agreement with data to look much better, but for the sake of clarity we have not added more lines to the figure, as long as the binning effect has already been illustrated in Fig. 6. Although in section one we have justified the use of the normalized couplings, we also show in Fig. 7 the result using universal couplings (dotted line). In this process, the effect of normalizing the couplings of the vector me-

son radiative decays is not as drastic as in Fig. 2 for the η decay where only the VMD mechanism was considered. In what follows we will only use the normalized couplings.

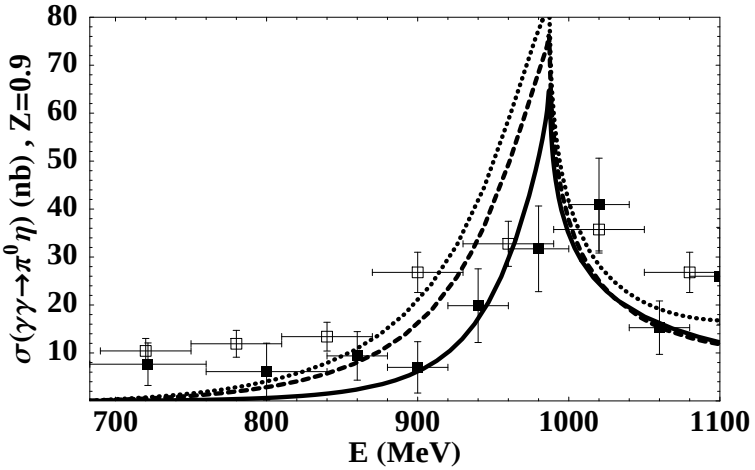

Figure 7: $\gamma\gamma \to \pi^0\eta$ cross section, using Eq. (9 (continuous line), adding the universal VMD contribution (dotted line) or the normalized VMD contribution (dashed line).

Second, in addition to the axial vector meson exchange in loops considered in the previous section, we have to include the loops with vector meson exchange for completeness. In fact, some of the uncertainties estimated in [5] were linked to these loops. For consistency, once again we have to sum the series obtained by iterating the loops in the four meson vertex shown in Fig. 8. Hence, the new amplitude, which we shall call t^{VMDL}, will be given by:

$$t^{VMDL} = t_{\eta\pi^0,\eta\pi^0}(M_I) G_{\eta\pi} \tilde{t}^{VMD}_{\eta\pi}(M_I) \left[\epsilon_1\epsilon_2 - \frac{(k_2\epsilon_1)(k_1\epsilon_2)}{k_1 k_2} \right] \tag{13}$$

where now $\tilde{t}^{VMD}_{\eta\pi}$ is the factor that multiplies the $\epsilon_1\epsilon_2$ product in the s-wave projection of the $t^{VMD}_{\eta\pi}$ amplitude in the $\gamma\gamma \to \pi^0\eta$ CM. Although the Lorentz structure of polarization vector products may seem rather complicated from Eq. (5), it is easy to show that after the s-wave projection the polarization vectors factorize indeed as $\epsilon_1\epsilon_2$. In a general frame the $\epsilon_1\epsilon_2$ factor has to be replaced by $\epsilon_1\epsilon_2 - (k_2\epsilon_1)(k_1\epsilon_2)/(k_1k_2)$. Once again we have factorized the amplitudes for the same reasons as done with the other terms.

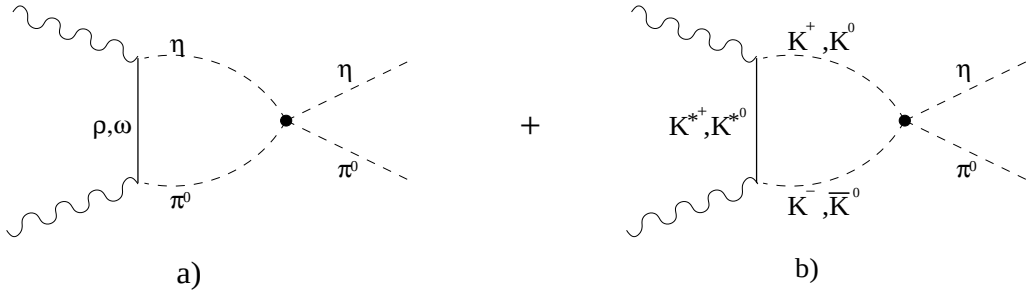

Figure 8: Loop diagrams for VMD terms. The diagrams with the two crossed photons are not depicted but are also included in the calculations.

Of course, when introducing loops with vector meson exchange we have to consider loops involving a K^{*+} or a K^{*0} exchanged between the photons (see Fig. 8.b), which were not present at tree level. These would be given by

$$t^{VMDL}_{K\bar{K}} = \Big(t_{\eta\pi^0,K^+K^-}(M_I)G_{K\bar{K}}(M_I)\tilde{T}^{VMD}_{K^+K^-}(M_I) + t_{\eta\pi^0,K^0\bar{K}^0}(M_I)G_{K\bar{K}}(M_I)\tilde{T}^{VMD}_{K^0\bar{K}^0}(M_I)\Big)\left[\epsilon_1\epsilon_2 - \frac{(k_2\epsilon_1)(k_1\epsilon_2)}{k_1k_2}\right] \quad (14)$$

The contribution of all these new VMD loop diagrams is an increase of the order of 10-20% of the result shown in Fig. 7 by the dashed line (normalized VMD couplings). The new result would overlap in a large region with the dotted line of Fig. 7 and hence we do not show it explicitly.

In what follows we make some considerations about the diagrammatic interpretation of the "all order" VMD calculation, the normalization of the $VP\gamma$ vertices and the meson-meson interaction. By "all order" VMD one means [5] that the full vector meson propagator $(s-M_V^2+iM_V\Gamma(s))^{-1}$ is used in the calculations. This full propagator includes self-energy diagrams in a Dyson-Schwinger resummation, leading to a shift of the bare mass and generating a width [41]. Thus, one must think in terms of self-energy insertions in the middle of the vector meson lines in Fig. 1 and 8. The $VP\gamma$ coupling normalization to agree with the radiative vector meson decays can also be understood as considering vertex correction diagrams in Fig.1 and 8, and therefore it does not lead to any double counting with the dressing of the vector meson propagator. Finally, the meson-meson interaction in the VMD terms leads to the diagrams of Fig. 8, in which the two pseudoscalar mesons interact through four-pseudoscalar meson vertices. The resummation of pseudoscalar meson-meson loops thus leaves apart the vector meson lines and the $VP\gamma$ vertices. Once again this ensures that there is no double counting.

3.3 Meson loops in $\eta \to \pi^0\gamma\gamma$

In the $\eta \to \pi^0\gamma\gamma$ case, the meson loop diagrams correspond to those of $\pi^0\eta \to \gamma\gamma$ but considering the π^0 as an outgoing particle. Hence, it is enough to replace $s = (p_\eta + p_\pi)^2$ by $M_I^2 = (p_\eta - p_\pi)^2 = (p_{\gamma_1} + p_{\gamma_2})^2$ in all the $\pi^0\eta \to \gamma\gamma$ amplitudes, which factorize in all the loop diagrams that we have considered so far, and in the $\tilde{t}_{\chi K}$ and $\tilde{t}_{AK^+K^-}$ function.

Since we are considering all the VMD diagrams and the chiral loops, we still have to take into account another kind of loop diagrams [5], shown in Fig. 9, which involve two anomalous $\gamma \to 3M$ vertices. Despite being $O(p^8)$ it has been found [5] that they can have a non negligible effect on the η decay. The further rescattering of the mesons in the diagrams of Fig. 9, given the structure of the γMMM vertex [5] in the momenta of the particles, would be suppressed by factors of $\vec{p}_\gamma^{\,2}/\vec{q}^{\,2}$ (with q the loop variable) with respect to those considered for the VMD mechanism. This, and the fact that these anomalous terms are already small, makes the consideration of rescattering in these loops superfluous. Therefore, it is enough to take the results from [5] where it is found that their largest contribution comes from the kaon loops. We use Eqs.(12),(13) and (27) of that reference (note that there is a global change of sign with respect to our notation). Concerning $\gamma\gamma \to \eta\pi^0$, these kind of loops have been neglected in the previous section, because the intermediate particles are very far off shell, due to the crossed character of the loop in the reaction.

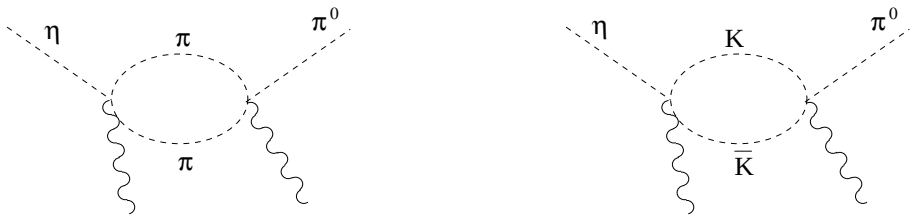

Figure 9: Diagrams with two anomalous $\gamma \to 3M$ vertices.

4 Results for $\eta \to \pi^0\gamma\gamma$

Using the model described in the previous sections, we plot in Fig. 10 the different contributions to $d\Gamma/dM_I$. We can see that the largest contribution is that of the tree level VMD (long dashed line). Let us recall that this is a new result as long as we are using the VMD couplings normalized to agree with the vector radiative decays. The resummation of the loops in Fig. 3 using Eq.(9), (short dashed line) gives a small contribution (0.011 eV in the total width), but when added coherently to the tree level VMD, leads to an increase of 30 % in the η decay rate (dashed-dotted line). More interestingly, the shape of the $\gamma\gamma$ invariant mass distribution is appreciably changed with respect to the tree level VMD, developing a peak at high invariant masses. The resummed VMD loops in Fig. 8, using Eqs.(13) and (14), leads, through interference, to a moderate increase of the η decay rate (double dashed dotted line), smaller than that of the chiral loops considered before. The last ingredient is the contribution of the anomalous mechanisms of Fig. 9 (continuous line), leading again to a moderate increase of the η decay rate, also smaller than the chiral loops from Eq.(9). These anomalous mechanisms have a very similar shape to the tree level VMD and interfere with it in the whole range of invariant masses.

Altogether, when integrating over the invariant mass, we get:

$$\Gamma(\eta \to \pi^0\gamma\gamma) = 0.47 \pm 0.08\,\text{eV}. \tag{15}$$

Note that the inclusion of the loops has increased the tree level VMD result by 50%. For comparison, we quote here what we would have obtained using the universal VMD couplings: 0.80 eV.

So far, the theoretical error has been obtained only from the propagation of the experimental errors in the vector meson radiative decay branching ratios, given in Table 1. The errors from this source had not been considered before although they will turn out to produce the largest uncertainty. In practice we generate a Gaussian weighted random value for each VMD coupling which yield a result for the width. This procedure is repeated a sufficiently large number of times, leading to an approximate Gaussian distribution of results from where we obtain a central value and the error.

We come now to revisit the uncertainties considered in [5]. One of the largest sources to the ± 0.2 eV accepted uncertainties in that work, was the contribution of the $a_0(980)$, whose sign was unknown. This problem is solved in the present work since the $a_0(980)$ is generated dynamically from the rescattering of the mesons implied in the Bethe-Salpeter resummation of the $t_{K^+K^-,\eta\pi^0}$ amplitude. Hence its effect can be easily observed comparing with the standard ChPT result, which is obtained by substituting the full $t_{K^+K^-,\eta\pi^0}$ by its lowest order $O(p^2)$. In Fig. 10 this corresponds to the difference between the continuous and the dotted line. The contribution of the $a_0(980)$ resonance tail is rather small

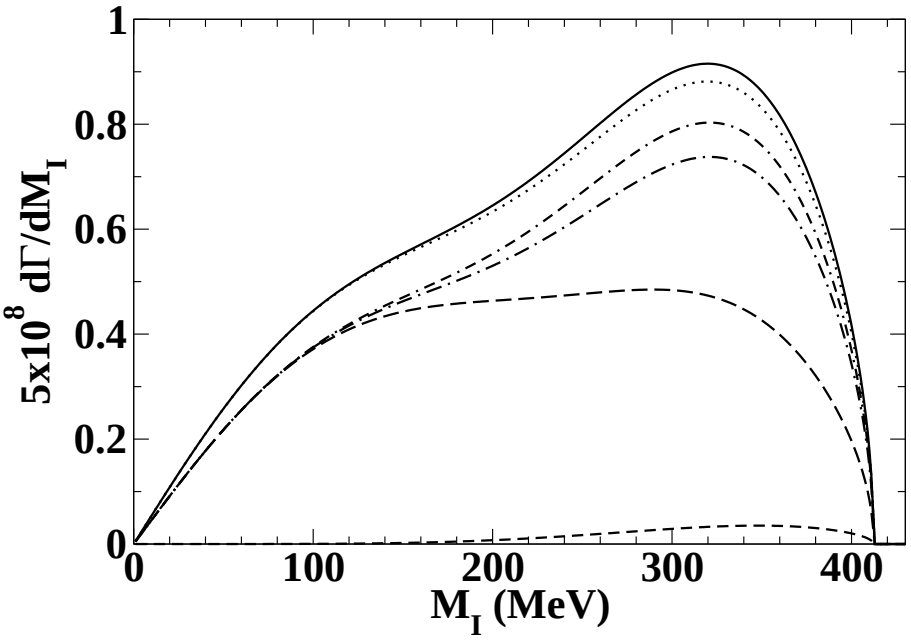

Figure 10: Contributions to the two photon invariant mass distribution. From bottom to top, short dashed line: chiral loops from Eq.(9); long dashed line: only tree level VMD; dashed-dotted line: coherent sum of the previous mechanisms; double dashed-dotted line: idem but adding the resummed VMD loops; continuous line: idem but adding the anomalous terms of Fig. 10, which is the full model presented in this work (we are also showing as a dotted line the full model but substituting the full $t_{K^+K^-,\eta\pi^0}$ amplitude by its lowest order).

and increases the η decay rate from 0.47eV to 0.48 eV. The sign of its contribution is unambiguously determined. Thus, the present calculation removes completely this source of error. The explicit calculation of the $a_0(980)$ contribution giving such a small effect justifies neglecting the $a_2(1320)$ resonance contribution which lies much further away in energy.

The other source of uncertainty in [5] was the contribution of the VMD loops. We have been able to calculate them in this work and, as seen in Fig. 10, these effects are also rather small. They increase the η decay rate by 0.02 eV. Altogether the $a_0(980)$ plus the VMD loops increase the η decay rate by 0.03 eV. We thus eliminate these two sources of previous uncertainties, while realizing at the same time that the uncertainties of 0.2 eV attributed to these sources in [5] were indeed a generous upper bound.

In our approach the tree level exchange of the $h_1(1170)$, $b_1(1235)$ and $h_1(1380)$ axial resonances [12] will be included as an uncertainty. The reason is that, according to [12], they would increase the decay width by about 0.07 eV. However, as shown in [12, 14], their inclusion in $\gamma\gamma \to \pi^0\pi^0$ with the couplings used in [12] would overestimate the $\gamma\gamma \to \pi^0\pi^0$ cross section. In view of these discrepancies, we thus consider safe to accept a theoretical uncertainty of the order of 0.05 eV which should still be a generous upper bound.

As commented at the beginning of section three, there are uncertainties due to isospin violating terms. We estimate the errors from this source using the results obtained in [5] for the G-parity violating term corresponding to Fig. 3 but with pion loops. This contribution is of the order of 0.05 eV to the total η decay rate.

Finally, by summing all errors in quadrature, we arrive to

$$\Gamma(\eta \to \pi^0\gamma\gamma) = 0.47 \pm 0.10\, eV \tag{16}$$

Note that although we have considered a new error source from the uncertainties in the vector radiative decays, which turns out to be the largest one, we still have reduced the uncertainty from previous calculations.

The result of Eq. (16) is in remarkable agreement with the latest experimental number [30], and lie within two sigmas from the earlier ones in [1, 2]. Confirmation of those preliminary results would therefore be important to test the consistency of this new approach. Furthermore, precise measurements of the $\gamma\gamma$ invariant mass distributions would be of much help given the differences found with and without loop contributions.

5 Conclusions

We have reanalyzed the $\eta \to \pi^0\gamma\gamma$ decay within the context of meson chiral lagrangians, gathering all the mechanisms discussed in the literature, but improving them in the following aspects:

On the one hand, using the well tested chiral unitary approach, we have removed the uncertainties from the $a_0(980)$ resonance as well as those from loops with the exchange of one vector meson. In particular, since the $a_0(980)$ is generated dynamically from the meson loop resummation, we have unambiguously determined the sign of its contribution, whereas for the one vector loops we have performed an explicit calculation that in previous works had only been considered as a large source of uncertainty.

On the other hand, we have also checked the consistency with other related processes: First, a relevant observation is that the tree level vector meson dominance amplitude with a universal SU(3) vector-vector-pseudoscalar coupling is not consistent with the $\rho \to \eta\gamma$, $\omega \to \pi^0\gamma$ and $\omega \to \eta\gamma$ decays. Consequently, throughout the $\eta \to \pi^0\gamma\gamma$ calculation, we have used couplings normalized to agree with the radiative vector meson decays. Second, we have established the consistency of our $\eta \to \pi^0\gamma\gamma$ model with the related $\gamma\gamma \to \eta\pi^0$ process.

Furthermore, we have performed a careful error analysis of our results. As a novelty we have considered the experimental errors in the vector meson radiative decay widths, which turn out to be the largest source of uncertainty. However, since, as just commented above, we have removed former sources of uncertainty, our final error is still smaller than previous estimates.

Altogether we have found a result of $\Gamma(\eta \to \pi^0\gamma\gamma) = 0.47 \pm 0.10\,\text{eV}$.

With the improved calculation just presented, it seems clear that the mechanisms thus far suggested in the literature in the context of meson chiral lagrangians lead to a result at variance with the experimental result $\Gamma = 0.84 \pm 0.18\,\text{eV}$ from [1, 2]. However, it is worth noticing the agreement of the above result with the new preliminary measurement $\Gamma = 0.42 \pm 0.14\,\text{eV}$ from [30]. Nevertheless, a measurement of the invariant mass distribution would be more stringent. Confirmation of the preliminary results of [30] and an accurate measurement of the $\gamma\gamma$ invariant mass distribution should be the experimental priorities to clarify the situation.

Acknowledgments

We are specially grateful to J.A. Oller for fruitful discussions, technical help and his careful reading of the manuscript. We would also like to acknowledge useful discussions with J. Bijnens. One of us, L.R., acknowledges support from the Consejo Superior de Investigaciones Científicas. J.R.P. acknowledges financial support from a CICYT-INFN collaboration grant as well as a Marie Curie fellowship MCFI-2001-01155. He also thanks the Dipartimento de Fisica, Universita' de Firenze-INFN Sezione di Firenze for its hospitality. This work is also partly supported by DGICYT contract numbers BFM2000-1326, PB98-0782, and the E.U. EURIDICE network contract no. HPRN-CT-2002-00311.

References

[1] D. Alde et al., Yad. Fiz 40 (1984) 1447; D. Alde et al., Z. Phys. C25 (1984) 225; L.G. Landsberg, Phys. Rep. 128 (1985) 301.

[2] K. Hagiwara *et al.* [Particle Data Group Collaboration], Phys. Rev. D **66** (2002) 010001.

[3] J. N. Ng and D. J. Peters, Phys. Rev. D **47** (1993) 4939.

[4] Y. Nemoto, M. Oka and M. Takizawa, Phys. Rev. D **54** (1996) 6777 [arXiv:hep-ph/9602253].

[5] L. Ametller, J. Bijnens, A. Bramon and F. Cornet, Phys. Lett. B **276** (1992) 185.

[6] S. Oneda and G. Oppo, Phys. Rev. 160 (1968) 1397.

[7] C. Picciotto, Nuovo Cim. A **105** (1992) 27.

[8] A. A. Bel'kov, A. V. Lanyov and S. Scherer, J. Phys. G **22** (1996) 1383 [arXiv:hep-ph/9506406].

[9] S. Bellucci and C. Bruno, Nucl. Phys. B **452** (1995) 626 [arXiv:hep-ph/9502243].

[10] J. Bijnens, A. Fayyazuddin and J. Prades, Phys. Lett. B **379** (1996) 209 [arXiv:hep-ph/9512374].

[11] M. N. Achasov *et al.*, Nucl. Phys. B **600** (2001) 3 [arXiv:hep-ex/0101043].

[12] P. Ko, Phys. Rev. D **47** (1993) 3933.

[13] P. Ko, Phys. Lett. B **349** (1995) 555 [arXiv:hep-ph/9503253].

[14] M. Jetter, Nucl. Phys. B **459** (1996) 283 [arXiv:hep-ph/9508407].

[15] T. Oest *et al.* [JADE Collaboration], Z. Phys. C **47** (1990) 343.

[16] D. Antreasyan *et al.* [Crystal Ball Collaboration], Phys. Rev. D **33** (1986) 1847.

[17] J. A. Oller and E. Oset, Nucl. Phys. A **620**, 438 (1997) [Erratum-ibid. A **652**, 407 (1997)].

[18] N. Kaiser, Eur. Phys. J. A **3** (1998) 307.

[19] J.A. Oller, E. Oset and J. R. Peláez, Phys. Rev. Lett. **80** (1998) 3452; Phys. Rev. D **59** (1999) 74001; Erratum-ibid.D60 (1990) 099906

[20] J. A. Oller and E. Oset, Phys. Rev. D **60** (1999) 074023.

[21] J. Nieves and E. Ruiz Arriola, Nucl. Phys. A **679** (2000) 57 [arXiv:hep-ph/9907469].

[22] A. Gomez Nicola and J. R. Pelaez, Phys. Rev. D **65** (2002) 054009 [arXiv:hep-ph/0109056].

[23] J. A. Oller and E. Oset, Nucl. Phys. A **629** (1998) 739 [arXiv:hep-ph/9706487].

[24] A. Dobado and J. R. Pelaez, Z. Phys. C **57** (1993) 501.

[25] H. Yamagishi and I. Zahed, Annals Phys. **247** (1996) 292 [arXiv:hep-ph/9503413].

[26] C. H. Lee, H. Yamagishi and I. Zahed, Nucl. Phys. A **653** (1999) 185 [arXiv:hep-ph/9806447].

[27] A. Bramon, R. Escribano, J. L. Lucio Martinez and M. Napsuciale, Phys. Lett. B **517** (2001) 345 [arXiv:hep-ph/0105179].

[28] J. E. Palomar, S. Hirenzaki and E. Oset, Nucl. Phys. A **707** (2002) 161

[29] E. Marco, S. Hirenzaki, E. Oset and H. Toki, Phys. Lett. B **470** (1999) 20 [arXiv:hep-ph/9903217].

[30] S. Prakhov, in Proceedings of the International Conference of Non-Accelerator New Physics, Dubna, Russia; B. M. Nefkens and J. W. Price, in the Eta Physics Handbook, Proc. of the Uppsala Workshop, http://www.tsl.uu.se∼faldt/eta/Proceedings.html, Published in Phys. Scripta **T99** (2002) 114 [arXiv:nucl-ex/0202008].

[31] J. Gasser and H. Leutwyler, Annals Phys. **158** (1984) 142.

[32] G. Ecker, J. Gasser, A. Pich and E. de Rafael, Nucl. Phys. B **321** (1989) 311.

[33] A. Bramon, A. Grau and G. Pancheri, Phys. Lett. B **283** (1992) 416.

[34] A. Bramon, A. Grau and G. Pancheri, Phys. Lett. B **344** (1995) 240.

[35] J. Bijnens and F. Cornet, Nucl. Phys. B **296** (1988) 557.

[36] J. F. Donoghue, B. R. Holstein and Y. C. Lin, Phys. Rev. D **37** (1988) 2423.

[37] H. Albrecht et al. Z. Phys.**C48** (1989) 183.

[38] J. F. Donoghue and B. R. Holstein, Phys. Rev. D **48** (1993) 137 [arXiv:hep-ph/9302203].

[39] T.Oest et al., Z. Phys. C47 (1990) 343.

[40] D. Antreasyan et al., Phys. Rev. D33 (1986) 1847.

[41] J. A. Oller, E. Oset and J. E. Palomar, Phys. Rev. D **63** (2001) 114009 [arXiv:hep-ph/0011096].